CHALMERS
UNIVERSITY OF TECHNOLOGY

Surface species and metal oxidation state during H2-assisted NH3-SCR of NOx over alumina-supported silver and indium

catalysts

MDPI

Article

Surface Species and Metal Oxidation State during H_2-Assisted NH_3-SCR of NO_x over Alumina-Supported Silver and Indium

Linda Ström *, Per-Anders Carlsson, Magnus Skoglundh and Hanna Härelind

Competence Centre for Catalysis, Department of Chemistry and Chemical Engineering, Chalmers University of Technology, SE-412 96 Göteborg, Sweden; per-anders.carlsson@chalmers.se (P.-A.C.); skoglund@chalmers.se (M.S.); hanna.harelind@chalmers.se (H.H.)

* Correspondence: linda.strom@chalmers.se; Tel.: +46-31-772-1000

Received: 1 January 2018; Accepted: 17 January 2018; Published: 19 January 2018

Abstract: Alumina-supported silver and indium catalysts are investigated for the hydrogen-assisted selective catalytic reduction (SCR) of NO_x with ammonia. Particularly, we focus on the active phase of the catalyst and the formation of surface species, as a function of the gas environment. Diffuse reflectance ultraviolet-visible (UV-vis) spectroscopy was used to follow the oxidation state of the silver and indium phases, and in situ diffuse reflectance infrared Fourier transform spectroscopy (DRIFTS) was used to elucidate the formation of surface species during SCR conditions. In addition, the NO_x reduction efficiency of the materials was evaluated using H_2-assisted NH_3-SCR. The DRIFTS results show that the Ag/Al_2O_3 sample forms NO-containing surface species during SCR conditions to a higher extent compared to the In/Al_2O_3 sample. The silver sample also appears to be more reduced by H_2 than the indium sample, as revealed by UV-vis spectroscopic experiments. Addition of H_2, however, may promote the formation of highly dispersed In_2O_3 clusters, which previously have been suggested to be important for the SCR reaction. The affinity to adsorb NH_3 is confirmed by both temperature programmed desorption (NH_3-TPD) and in situ DRIFTS to be higher for the In/Al_2O_3 sample compared to Ag/Al_2O_3. The strong adsorption of NH_3 may inhibit (self-poison) the NH_3 activation, thereby hindering further reaction over this catalyst, which is also shown by the lower SCR activity compared to Ag/Al_2O_3.

Keywords: lean NO_x reduction; silver-alumina; indium-alumina; ammonia-SCR; hydrogen effect

1. Introduction

The development of fuel-efficient engines, operating under lean conditions, is motivated by fluctuating oil prices, more stringent emission legislations, and climate changes. Among the most attractive exhaust aftertreatment techniques for lean NO_x reduction is the selective catalytic reduction with either ammonia (NH_3-SCR) or hydrocarbons (HC-SCR). For example, Cu-based zeolites have recently been shown to exhibit high NO_x removal activity in a wide temperature range [1–3]. In contrast to NH_3-SCR, the HC-SCR catalysts need to be further improved as to be competitive. This puts pressure on building new understanding of the materials and mechanisms for HC-SCR. It seems, though, that NH_3 is a key intermediate for both techniques [4,5]. Due to its excellent thermal and mechanical stability, alumina is the most widely used catalyst support material [6]. The silver-alumina system has been studied for HC-SCR applications and with the pioneering work by Satokawa [7] in 2000, it was shown that the catalytic activity for NO_x reduction can be further improved by the addition of small amounts of hydrogen. This widely studied phenomenon [8–11] is denoted the 'hydrogen effect' and has previously been regarded as limited to silver-based catalysts only [12]. However, recently In/Al_2O_3, which also has been studied for SCR applications [13–19], was found to exhibit a hydrogen

effect, albeit to a lower extent compared to Ag/Al_2O_3 [20]. The hydrogen effect over Ag/Al_2O_3 has been suggested to originate from the reduction of adsorbed nitrogen species [10,21,22], changes in the type of Ag species [23–25], and/or enhanced activation of the reductant [9,11]. However, in contrast to other precious metal catalysts, alumina-supported silver is not active for H_2-SCR [26]. From a practical point of view, H_2 can be provided to the vehicle's exhaust after treatment by on-board reforming of for example solid amine salts or fuel [19,27].

Several studies have focused on the role of silver phases in the Ag/Al_2O_3 catalyst [28–33], suggesting the active phase for the selective reduction of NO_x to be $Ag_n{}^{\delta+}$-clusters [32,33] and Ag^+ ions [28,29], or a combination of these. Except for these species, metallic silver (Ag^0) is recognized as responsible for complete combustion of the reductant [34]. In the In/Al_2O_3 catalyst, highly dispersed indium cluster sites (In^{3+}) have been identified as the active component for hydrocarbon activation during HC-SCR [17].

A deeper understanding of the underlying mechanisms of the hydrogen effect is useful, not only to improve the SCR catalysts, but also for facilitating development of systems that reduce NO_x efficiently without the addition of hydrogen. In this study, we compare Ag/Al_2O_3 and In/Al_2O_3 catalysts, for the SCR of NO_x with ammonia as model reductant. In particular, we are focusing on how the catalytically active silver and indium phases are affected by the SCR environment, and how the formed surface species interact with these phases, using diffuse reflectance ultraviolet-visible (UV-vis) spectroscopy, in situ diffuse reflectance infrared Fourier transform spectroscopy (DRIFTS), and ammonia-temperature programmed desorption (NH_3-TPD).

2. Results

In this study, we compared H_2-assisted NH_3-SCR of NO_x over Ag/Al_2O_3 and In/Al_2O_3. In Section 2.1, we show the NO_x conversion and formed species during the SCR experiments. In addition, we compare the density of acidic sites by NH_3-TPD (Section 2.2). We have also focused on the possible changes in the active phase and surface species as a function of gas phase components. These results are presented in Sections 2.3 and 2.4

2.1. Catalytic Activity

The Ag/Al_2O_3 and In/Al_2O_3 samples were evaluated as NH_3-SCR catalysts using a flow reactor with a feed composition of 500 ppm NO, 500 ppm NH_3, 10% O_2, 5% H_2O, and Ar as carrier gas. The experiments were subsequently repeated with the addition of 1000 ppm H_2.

The NO_x reduction and NH_3 conversion, as well as the formation of NO_2 and N_2O over Ag/Al_2O_3, are shown in Figure 1. Without the addition of H_2, the catalyst is inactive for NO_x reduction. However, H_2-assisted NH_3-SCR reduces NO_x in a broad temperature window and with a maximum reduction just above 80%. The selectivity towards N_2 is high, in accordance with previous reports [35,36], 80% when H_2 is present in the feed. It can also be seen that the low N_2O formation decreases even further when H_2 is present, confirming the results of Kondratenko et al., that H_2 suppresses the total N_2O production [25]. This is assigned to H_2-induced Ag^0 formation, which likely is responsible for the N_2O decomposition [37]. The negative values of NO_x reduction above 350 °C observed when H_2 is absent (black line in Figure 1a) is likely due to the oxidation of NH_3 to NO, which also explains the significant amount of NH_3 converted in Figure 1b [35]. Shimizu and Satsuma [32] suggest that the addition of H_2 to $NH_3 + O_2$ enhances the oxidative activation of NH_3 by decreasing the activation energy of the rate-determining step, (i.e., formation of NH_x).

The In/Al_2O_3 catalyst is, like Ag/Al_2O_3, inactive for NO_x reduction with solely NH_3, as seen in Figure 2. With the addition of H_2, the NO_x reduction clearly increases, however, to a considerably lower level compared to Ag/Al_2O_3. In order to separate between the effect of the active phase and the Al_2O_3 support, the equivalent experiments were executed for γ-Al_2O_3, which is totally inactive for both the NO_x reduction and NH_3 conversion, even with addition of H_2 (results not shown), in accordance with the findings of Doronkin et al. [19].

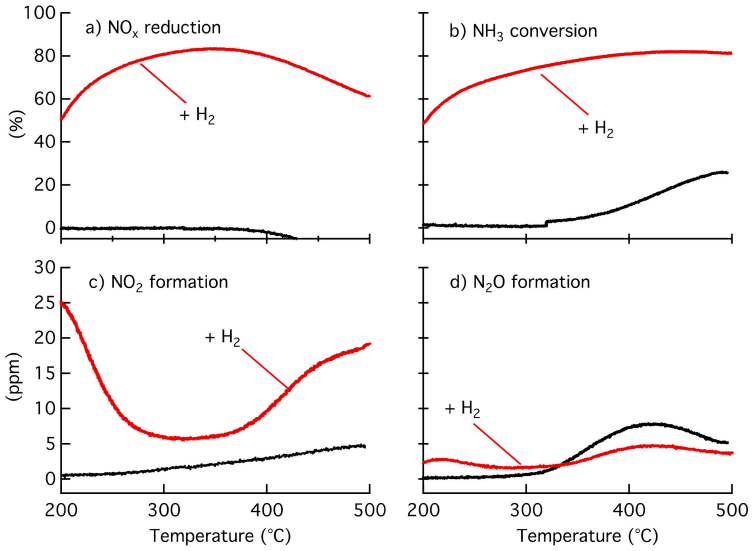

Figure 1. NH_3-SCR over Ag/Al_2O_3. (**a**) NO_x reduction; (**b**) NH_3 conversion; (**c**) NO_2 formation and (**d**) N_2O formation over the Ag/Al_2O_3 catalyst as a function of temperature. Inlet gas composition: 500 ppm NO, 500 ppm NH_3, 10% O_2 and 5% H_2O, Ar-bal. (red lines represents the addition of 1000 ppm H_2).

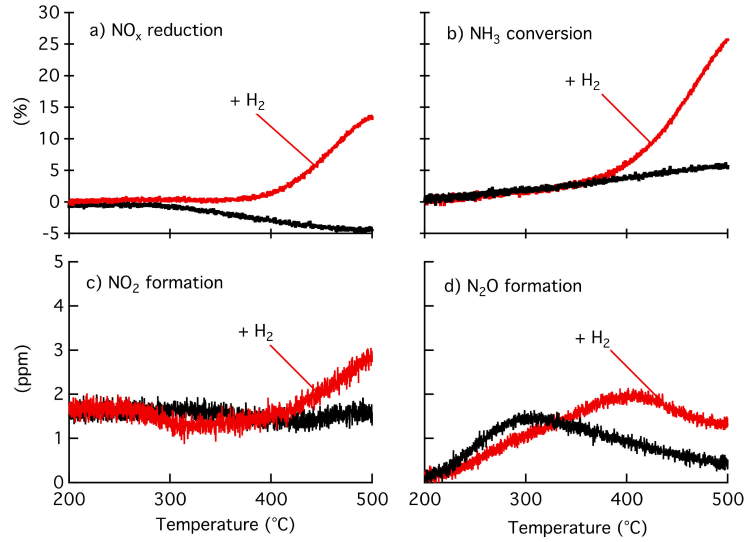

Figure 2. NH_3-SCR over In/Al_2O_3. (**a**) NO_x reduction; (**b**) NH_3 conversion; (**c**) NO_2 formation and (**d**) N_2O formation over the In/Al_2O_3 sample as a function of temperature. Inlet gas composition: 500 ppm NO, 500 ppm NH_3, 10% O_2 and 5% H_2O, Ar-bal. (red lines represents the addition of 1000 ppm H_2).

2.2. Surface Acidity

The surface of the alumina support consists of a combination of aluminum and oxygen ions, which may exhibit lower coordination numbers compared to ions of the bulk. The surface ions hold vacant sites, which, at ambient temperature, are always occupied by either dissociatively adsorbed water in the form of surface hydroxyl (OH) groups, or by coordinated water molecules [38]. Twelve different configurations of OH can be present at the surface, bearing slightly different net charges, consequently possessing different properties, such as variations in acidity [39,40].

Ammonia-TPD experiments were performed in order to investigate the surface acidity of the samples. The desorption profiles of NH_3 during the NH_3-TPD measurements over the γ-Al_2O_3, Ag/Al_2O_3 and In/Al_2O_3 samples, are shown in Figure 3. The total amount of desorbed ammonia,

summarized in Table 1, shows that the highest concentration of acidic sites is found for the γ-Al_2O_3 sample, followed by In/Al_2O_3 and Ag/Al_2O_3, which possessed the lowest concentration of acidic sites. Comparing the NH_3 desorption peaks for the samples; the weakest type of acidic site (i.e., the peak with lowest desorption temperature) is found at a higher temperature for the γ-Al_2O_3 sample, corresponding to 19% of the total desorbed amount of NH_3, compared to the Ag/Al_2O_3 (49%) and In/Al_2O_3 (16%) samples, respectively. The peak representing the strongest type of acidic site, i.e., the peak at the highest temperature, is also found at a higher temperature for the γ-Al_2O_3 sample. In addition, the highest desorption-temperature peak of the impregnated samples corresponds to the middle-temperature desorption peak of γ-Al_2O_3, indicating that the impregnation with silver and indium, respectively, results in less strong acidity for these samples. For the γ-Al_2O_3 sample, 33% of the total desorbed amount of NH_3 is adsorbed on this (strongest acidic) type of site, compared to 6% in the Ag/Al_2O_3 and 52% in the In/Al_2O_3 sample. However, the Gaussian peak representing the strongest acidic sites of the γ-Al_2O_3 sample is centered around almost 100 °C higher temperature compared to the peak holding the most acidic site of In/Al_2O_3. This implies that the impregnation procedure of γ-Al_2O_3 leads to an electronical modification and physical blockage of acidic sites at the catalyst support.

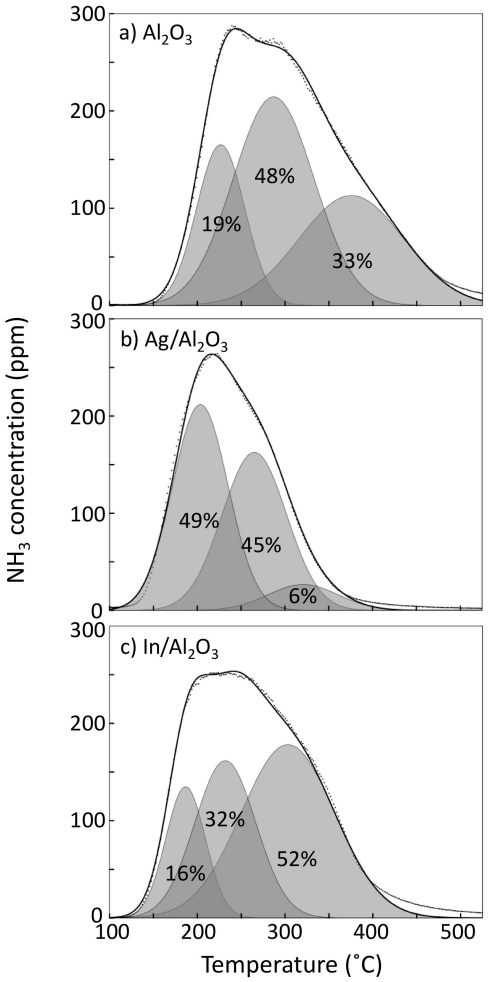

Figure 3. NH_3-temperature programmed desorption (TPD) profiles for (**a**) γ-Al_2O_3; (**b**) Ag/Al_2O_3 and (**c**) In/Al_2O_3, with the desorbed NH_3 concentration as a function of the temperature. The desorbed amount of NH_3 in the deconvoluted peaks are denoted in percentage of the measured total desorbed amount of NH_3.

Table 1. Total desorbed amount of NH_3 during the NH_3-TPD experiments.

Sample	Desorbed NH_3 (mmol/cm^2)
γ-Al_2O_3	11.2
Ag/Al_2O_3	7.4
In/Al_2O_3	9.5

2.3. Characterization of the Oxidation State of the Active Phase

Silver and indium species present in the catalyst samples were characterized using diffuse reflectance UV-vis spectroscopy. In order to investigate the influence of the NH_3-SCR reaction components, the samples were pretreated with NO, NH_3 and H_2, respectively. The UV-vis spectrum of the fresh (i.e., non-pretreated) Ag/Al_2O_3 sample (alumina subtracted) is shown in Figure 4, with absorbance peaks assigned according to Table 2. The spectrum shows that the sample contains a mixture of isolated Ag^+-ions, $Ag_n{}^{\delta+}$-clusters and Ag^0. Note that some isolated Ag^+-ions, which exhibited peaks below 200 nm, may have been present in the samples without being detected, since the spectrum only contained signals above 200 nm due to instrument limitations [41].

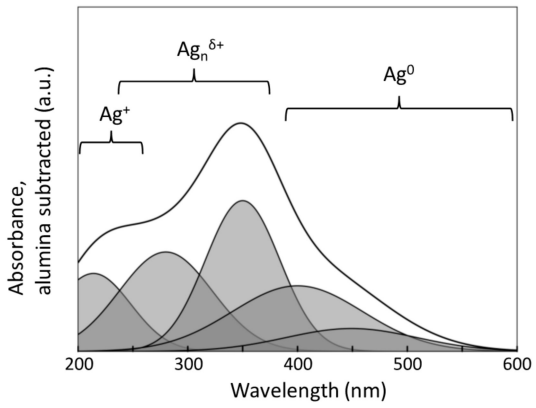

Figure 4. Ultra-violet (UV)-vis spectrum of the fresh (i.e., non-pretreated) Ag/Al_2O_3 sample, with the absorbance for the alumina sample subtracted, as a function of the wavelength. The peak ranges assigned to isolated Ag^+-ions, $Ag_n{}^{\delta+}$-clusters and Ag^0 are denoted.

Table 2. Assignment of absorption peaks in the UV-vis spectra of Ag/Al_2O_3.

Species	Wavelength [nm]	Reference
Isolated Ag^+-ions	192–250	[32]
	196, 212, 224	[42]
	220	[43]
	215–240	[44]
	212, 260	[44]
$Ag_n{}^{\delta+}$-clusters	260–370	[37]
	238–272	[45,46]
	322	[42]
	350, 285	[32]
Ag^0	>390	[28,29,32,42,46–48]

Figure 5 shows, in the same scale as Figure 4, the UV-vis spectra of the Ag/Al_2O_3 sample after pretreatments in H_2, NO and NH_3 at 300 °C. The H_2 pretreatment results in increased intensity of the bands at wavelengths corresponding to $Ag_n{}^{\delta+}$-clusters and metallic silver, as shown in Figure 5a. In contrast, the absorption spectrum recorded after pretreatment in NO (Figure 5b) shows decreased

intensity, compared to the fresh sample, at wavelengths corresponding to $Ag_n^{\delta+}$-clusters and metallic silver, indicating that NO slightly oxidizes the catalyst surface at 300 °C. In Figure 5c, the spectrum recorded after NH_3-pretreatment shows that the surface is reduced by NH_3. Compared to the fresh sample, this pretreatment shifts peaks from clusters to more completely reduced Ag phases.

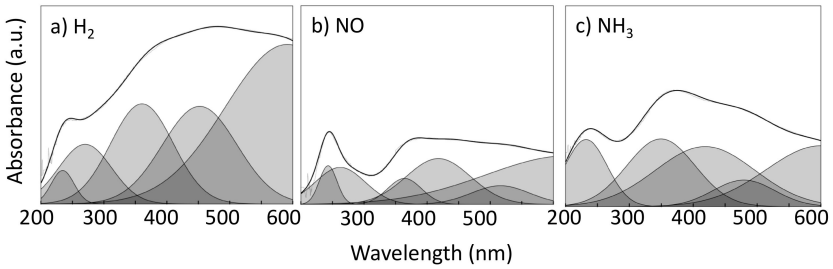

Figure 5. UV-vis spectra for the Ag/Al_2O_3 sample, with the absorbance for the alumina sample subtracted, plotted as a function of the wavelength. The graphs represent the spectra after pretreatment in (**a**) H_2, (**b**) NO, and (**c**) NH_3 at 300 °C. The scale of these figures is the same as of Figure 4.

The UV-vis spectrum of the fresh (i.e., non-pretreated) In/Al_2O_3 sample is shown in Figure 6. Absorption peaks in the range 200–450 nm are assigned to In_2O_3 [49–54]. Lv et al. [49] experienced that increased concentration of In_2O_3 results in a broadening and a redshift of the absorbance edge. The spectrum recorded after the H_2-pretreatment shows broadened absorption peaks with a slight redshift (see Figure 7a). However, peaks at wavelengths above 450 nm increases somewhat after the H_2-pretreatment, indicating the presence of more reduced indium species. Increased and broadened absorption peaks in the range 200–450 nm are detected after pretreatments also with NO and NH_3 at 300 °C (see Figure 7b,c), which could indicate increased In_2O_3 concentration in the sample.

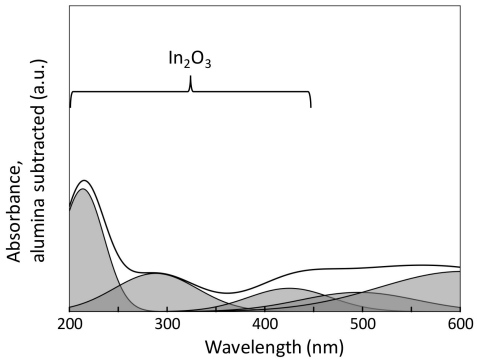

Figure 6. UV-vis spectrum of the fresh (i.e., non-pretreated) In/Al_2O_3 sample, with the absorbance for the alumina sample subtracted, as a function of the wavelength. The peak range assigned to In_2O_3 is denoted.

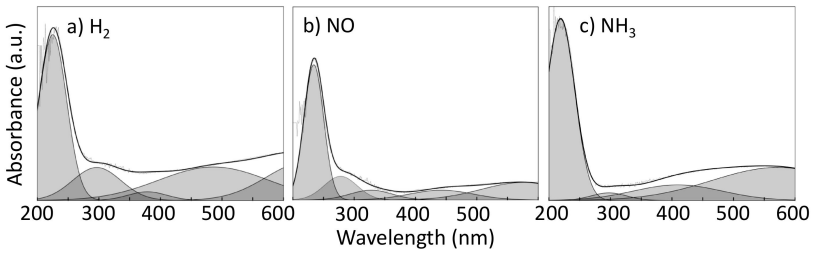

Figure 7. UV-vis spectra for the In/Al_2O_3 sample, with the absorbance for the alumina sample subtracted, plotted as a function of the wavelength. The graphs represent the spectra after pretreatment in (**a**) H_2, (**b**) NO, and (**c**) NH_3 at 300 °C. The scale of these figures is the same as of Figure 6.

2.4. Evaluation of Surface Species

The gas environment influences the surface of the catalyst, and in order to study the active phase and connect that to the reaction itself, DRIFTS was used to follow the formation of surface species at reaction conditions. Figure 8 shows the formation of surface species for the Ag/Al_2O_3, In/Al_2O_3 and γ-Al_2O_3 samples during exposure to NO, NH_3, H_2 and O_2 at 300 °C. The measurements were performed after 10 min exposure to the gas mixture in the last measurement sequence (see Table 3). All observed peaks remained after the specific gas component that gave rise to the corresponding absorption band, was switched off. This indicates that the surface species are chemisorbed to the samples. Below, absorption bands assigned to the adsorption of NO and NH_3 are presented separately. Also, absorption bands assigned to hydroxyl groups (i.e., bands at 3500–3800 cm^{-1} [55]) were observed (Figure 8). Comparing the relative peak intensities within the OH-band area of the infra-red (IR) patterns, it can be shown that the spectrum of the γ-Al_2O_3 sample resembled the one of In/Al_2O_3 more closely, compared to Ag/Al_2O_3.

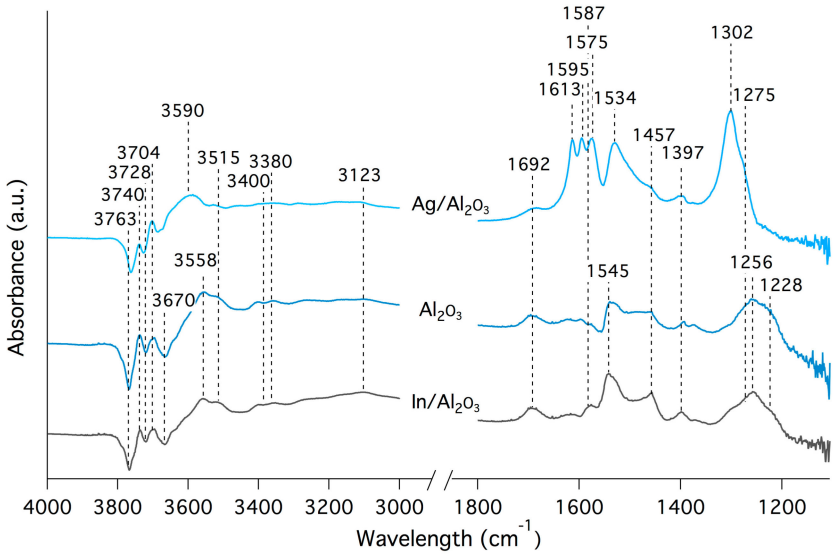

Figure 8. Diffuse reflectance infrared Fourier transform spectroscopy (DRIFTS) spectra showing formation of surface species for the Ag/Al_2O_3, In/Al_2O_3 and γ-Al_2O_3 samples during the exposure to selective catalytic reduction (SCR) reaction conditions (NO, NH_3, H_2, O_2, Ar-bal.) at 300 °C.

Table 3. The seven DRIFTS sequences. Gas condition: 500 ppm NO, 1000 ppm H_2 and 500 ppm NH_3. All sequences included 10% O_2 and Ar as the carrier gas.

Sequence	NO	H_2	NH_3
1	NO		
2	NO	H_2	
3	NO	H_2	NH_3
4		H_2	NH_3
5			NH_3
6	NO		NH_3
7	NO	H_2	NH_3

2.4.1. Assignment of NO Absorption Bands

Exposing Al_2O_3-based catalysts to NO and O_2 (or to NO_2) leads to the formation of surface nitrate and nitrite species. Nitrites have been recognized as an intermediate state in the formation of nitrates over Ag/Al_2O_3 [21], which may be a reason for the nitrite band to appear at 1228 cm^{-1} in the γ-Al_2O_3 and In/Al_2O_3 spectra, but not in the spectrum of Ag/Al_2O_3. Absorption bands related to the

symmetric N=O stretching vibrations are located in the region between 1650 and 1500 cm^{-1}, while the asymmetrical stretching of the O–N–O group can be detected between 1200 and 1350 cm^{-1} [21,34,56]. The spectra of In/Al_2O_3 and γ-Al_2O_3 exhibit broad peaks centered around 1256 cm^{-1}, as shown in Figure 8. This band is assigned to (bidentate) nitrate [57]. In the same region, at 1302 cm^{-1}, Ag/Al_2O_3 exhibits a sharp peak, which is assigned to monodentate nitrate [21,57]. The three peaks located at 1575, 1595 and 1613 cm^{-1} for the Ag/Al_2O_3 sample are assigned to bridged-, bidentate- and mono-dentate nitrate, respectively [21,41]. A summary of all absorption band assignments upon NO exposure is found in Table 4.

Table 4. Assignments of infra-red (IR) peaks associated with nitrite and nitrate species.

Wavenumber (cm^{-1})	Appears in Sample	Surface Species	References
1228	Al_2O_3, In/Al_2O_3	Nitrite	[21]
1256	Al_2O_3, In/Al_2O_3	Bidentate nitrate	[21,58]
1302	Ag/Al_2O_3	Monodentate nitrate	[21]
1534	Ag/Al_2O_3	Monodentate nitrate	[21]
1545	Al_2O_3, In/Al_2O_3	Monodentate nitrate	[21]
1575	Ag/Al_2O_3	Monodentate nitrate	[21]
1595	Ag/Al_2O_3	Bidentate nitrate	[21]
1613	Ag/Al_2O_3	Bridged nitrate	[21,59,60]

2.4.2. Assignment of NH_3 Absorption Bands

The symmetric and asymmetric vibration of surface coordinated NH_3 results in absorption bands at 1275 and 1587 cm^{-1}, respectively [61]. Moreover, the bands at 1397 and 1692 cm^{-1} are likely due to the adsorption of NH_4^+ ions at Brønstedt acidic sites [61,62]. The less pronounced absorption bands at 3380 and 3400 cm^{-1} are assigned to the symmetric and asymmetric N–H stretching vibrations of NH_3 hydrogen bonded to surface OH [62,63]. A summary of the absorption bands associated with ammonia is found in Table 5.

Table 5. Assignments of IR peaks associated with ammonia surface species.

Wavenumber (cm^{-1})	Vibration	Reference
1275	Symmetric bending of surface coordinated NH_3	[61]
1397	NH_4^+ ions at Brønstedt acidic site	[62,63]
1587	Asymmetric bending of surface coordinated NH_3	[61]
1692	NH_4^+ ions at Brønstedt acidic site	[62,63]
3380	Symmetric NH stretching vibrations of NH_3 hydrogen bonded to surface OH	[62,63]
3400	Asymmetric NH stretching vibrations of NH_3 hydrogen bonded to surface OH	[63]

3. Discussion

The NH_3-SCR results (Figures 1 and 2) show that the H_2-assisted reduction of NO at 300 °C is high over the Ag/Al_2O_3 sample and low over the In/Al_2O_3 sample. In situ DRIFTS results (Figure 8) show that the formation of NO-containing species is higher over the Ag/Al_2O_3 sample compared to the In/Al_2O_3 and γ-Al_2O_3 samples at this temperature. An efficient adsorption of the gas phase species is crucial for achieving an effective catalytic conversion. However, all absorption bands assigned to NH_3 adsorption are more pronounced for the γ-Al_2O_3 and In/Al_2O_3 samples, compared to the Ag/Al_2O_3 sample. This indicates that the adsorption of NH_3-surface species is more efficient over the former two samples compared to the latter, which is supported by the NH_3-TPD (Figure 3), showing that the γ-Al_2O_3 and In/Al_2O_3 samples provide higher density of acidic sites, compared to the Ag/Al_2O_3 sample. Furthermore, the DRIFTS spectra show differences at the wavelengths corresponding to OH-groups. The In/Al_2O_3 pattern resembles the one of γ-Al_2O_3 to a higher degree compared to Ag/Al_2O_3. Since alumina is impregnated with Ag and In in equivalent molar amounts, this implies

that Ag affects the acidic properties of the OH-rich alumina surface to a higher degree compared to In, resulting in a lower concentration of acidic sites for Ag/Al_2O_3.

Silver clusters ($Ag_n^{\delta+}$) have previously been identified as the prime species for the activity in H_2-assisted NH_3-SCR [64], and it has been shown that the activity is linearly proportional to the relative amount of these clusters [32]. Shimizu and Satsuma [32] suggest the following reaction mechanism for H_2-NH_3-SCR over Ag/Al_2O_3: (i) dissociation of H_2 on the Ag site, (ii) spillover of H^+ to form a proton on Al_2O_3, (iii) aggregation of isolated Ag^+ ions to $Ag_n^{\delta+}$-clusters ($n \leq 8$), (iv) reduction of O_2 promoted by $Ag_n^{\delta+}$-clusters and H^+ to O_2^-, H_2O and $Ag_n^{(\delta+x)+}$ or Ag^+, (v) N–H activation by O_2^- to yield NH_x ($x \leq 2$) (vi) oxidation of NO by O_2^- forming NO_2, (vii) reaction between NH_x and NO to yield N_2 and H_2O. The study by Tamm et al. [65] confirms that silver is needed for the dissociation of H_2, which directly participates in the reaction mechanism and also that the NO to NO_2 oxidation is part of this mechanism.

The UV-vis spectra of the In/Al_2O_3 sample show increased peak intensity for bands assigned to In_2O_3 but also increased absorbance at higher wavelengths (>450 nm) after pretreatment in H_2. The reaction mechanism of H_2-assisted NH_3 over In/Al_2O_3 could therefore resemble what Shimizu et al. suggested for Ag/Al_2O_3. However, the NH_3-TPD profiles of the catalysts elucidate the difference in acidity between the catalysts, where the In/Al_2O_3 sample contains significantly stronger acidic sites compared to the Ag/Al_2O_3 sample. An important difference in the mechanisms between the two catalysts could therefore be the stronger affinity between NH_3 and In/Al_2O_3, possibly hindering the NH_3 activation and thereby hindering further reaction over this catalyst to a higher extent compared to Ag/Al_2O_3. Another possible issue that may restrain the NO_x conversion over In/Al_2O_3 is the lower adsorption of NO species at the catalyst surface.

4. Materials and Methods

4.1. Catalyst Preparation and Basic Characterization

Two catalyst samples, 2.0 wt % Ag/Al_2O_3 and 2.1 wt % In/Al_2O_3 (which corresponds to equivalent molar amount of Ag and In, respectively), were prepared by incipient wetness impregnation of γ-Al_2O_3 (PURALOX®SBa 200, Sasol, Hamburg, Germany) using freeze-drying, according to the procedure described in detail previously [20], and briefly below. Silver nitrate (≥99.0% Sigma-Aldrich/Merck, Darmstadt, Germany) and indium nitrate hydrate (99.99% Sigma-Aldrich) were used as the active phase precursor for Ag and In, respectively. After impregnation, the samples were frozen in liquid nitrogen, subsequently freeze-dried, and finally calcined in air at 600 °C for four hours. The as prepared powder samples were characterized with respect to surface area by N_2 sorption (BET) and crystal structure by X-ray diffraction (XRD), as described in details elsewhere [20].

For the evaluation of the catalytic activity for NH_3-SCR, monolith samples with 188 channels (400 CPSI, $\varnothing$ = 20 mm, L = 20 mm) were cut from a commercial cordierite honeycomb structure (Corning, Corning, NY, USA) and calcined in air at 600 °C for one hour. Binder agent (DISPERAL® P2, Sasol) and one of the powder catalysts (ratio 1:4) in 1:1-ratio ethanol-water solutions were mixed to form washcoat slurries. The monoliths were dipped into the slurries, gently shaken for removal of excess slurry, dried (90 °C in air), and subsequently calcined (500 °C, 3 min). The coating procedure was repeated until the washcoat mass corresponded to 20% of the coated monolith mass. Finally, the monolith samples were calcined in air (600 °C, 1 h).

The catalyst samples have previously been characterized with respect to surface area and crystal structure [20]. The specific surface areas are 197, 185, and 188 m^2/g, for γ-Al_2O_3, Ag/Al_2O_3 and In/Al_2O_3, respectively. X-ray diffractograms indicate that the main crystalline phase in all samples is γ-Al_2O_3, and other crystalline phases (if any) are only present as particles smaller than 3–5 nm [66], in line with previous studies [17,18].

4.2. Lean NO_x Reduction Experiments

The catalytic activity for NH_3-SCR was evaluated in extinction experiments (500–100 °C, 10 °C/min) at a flow rate of 3500 mL/min (GHSV of 33,400 h^{-1}) in a flow reactor setup previously described by Kannisto et al. [67]. Briefly, the reactor consisted of a horizontal quarts tube (L = 80 cm, $Ø_i$ = 22 mm) heated by a metal coil. The catalyst sample was positioned close to the tube outlet, surrounded by bare monoliths for shielding of heat radiation to the thermocouples [68], which were placed inside and just before the coated monolith. Prior to each measurement, the sample was pretreated in 10% O_2 (Ar-balance) at 500 °C for 30 min. During the experiments, the gas composition was 500 ppm NO, 500 ppm NH_3, 10% O_2, and 5% H_2O, in the presence or absence of 1000 ppm H_2 (Ar-balance). The outlet gas composition was analyzed by a gas phase Fourier transform infrared (FTIR) spectrometer (MKS 2030, MKS Instruments, Telford, UK). The reduction of NO_x and conversion of NH_3 were obtained from the ratios of the differences between the inlet and outlet concentrations to the corresponding inlet concentration.

4.3. UV-Vis Spectroscopy

The samples, pretreated in varying SCR gas components, were characterized by diffuse reflectance UV-vis spectroscopy. Reflectance spectra in the wavelength range 200–1200 nm were recorded using a Varian Cary 5000 UV-vis near-IR (NIR) spectrophotometer, equipped with an external DRA-2500 unit (Agilent, Santa Clara, CA, USA). The same flow reactor equipment as in the NO_x reduction experiments was used for the pretreatments, where the samples were exposed to NO (1500 ppm, Ar balance), NH_3 (1500 ppm, Ar balance), and H_2 (3000 ppm, Ar balance), respectively. The pretreatments were carried out in a gas flow of 100 mL/min for 20 min at 300 °C. During data processing, the spectrum of the alumina support (which was pretreated in the same way as the Ag/Al_2O_3 and In/Al_2O_3 samples) was subtracted, and each spectrum was deconvoluted using Gaussian peaks for evaluation purposes.

4.4. In Situ DRIFTS

The surface species on the samples were characterized during SCR reaction conditions by in situ DRIFTS. The instrument used was a Bruker Vertex70 spectrometer equipped with a high-temperature reaction cell (Harrick Scientific, Pleasantville, NY, USA) with KBr windows. Prior to the measurements, the samples were pressed into tablets and then crushed by a mortar, in order to enlarge the powder particles to avoid channeling during the measurement. Subsequently, the powder fraction of the crushed tablets was sieved to a size range of 38 to 75 µm.

After placing the sample in the reaction cell, the Ag/Al_2O_3 and In/Al_2O_3 samples were pretreated at 500 °C in NO (2000 ppm, Ar-bal.) for 30 min, followed by O_2 (10%, Ar bal.) for 45 min, and finally H_2 (1000 ppm, Ar bal.) for 15 min. The γ-Al_2O_3 sample was pretreated in O_2 (10%, Ar bal.) for 45 min and then H_2 (1000 ppm, Ar bal.) for 15 min. The gas conditions during the measurement sequence is listed in Table 3, and corresponded to 500 ppm NO, 500 ppm NH_3, 1000 ppm H_2, and 10% O_2 (Ar balance). Each sequence lasted for 10 min and data were collected a few seconds after starting the experiment, after 5 min, and finally after 10 min. A resolution of 1 cm^{-1} was adapted, and 128 scans were recorded for the background spectra (recorded in Ar at 300 °C), and 64 scans for the measurements. All experiments were carried out at 300 °C in a flow rate of 100 mL/min and the data are presented as absorbance ($\log I/R$).

4.5. NH_3-TPD

The concentration and strength of acidic sites of the coated monolith samples were measured by NH_3-TPD. The flow reactor presented in Section 2.2 was used for this purpose, where the sample first was pretreated in 10% O_2 (20 min) in order to remove carbonaceous matter, flushed with argon (5 min), and then exposed to 1000 ppm H_2 (20 min) at 550 °C. During the following NH_3-TPD experiment, the catalyst surface was exposed to NH_3 (1000 ppm) at 100 °C until saturation, followed by Ar

flushing until the NH_3 signal vanished. The temperature was subsequently increased linearly to 550 °C (20 °C/min) while the desorbed NH_3 was measured continuously. For peak identification purposes, the NH_3-TPD profiles obtained are deconvoluted into Gaussian peaks.

5. Conclusions

This work shows that NO-species are formed to a higher extent over Ag/Al_2O_3 during SCR conditions, compared to In/Al_2O_3. The latter provide higher density of acidic sites, quantified by NH_3-TPD, and also exhibit higher NH_3 adsorption, as shown by DRIFTS. Moreover, the Ag/Al_2O_3 sample is more clearly reduced by H_2, compared to In/Al_2O_3. However, H_2 seems to promote the formation of highly dispersed In_2O_3 clusters, which previously have been suggested to be crucial for HC-SCR and could be important for the activation of the reducing agent also during H_2-assisted NH_3-SCR. Since adsorption of reactants in suitable proportions is crucial for high catalytic activity, an important difference between the two catalysts could be the stronger affinity for NH_3 over In/Al_2O_3, compared to Ag/Al_2O_3. This can possibly inhibit the NH_3 activation over the former, and thereby hindering further reaction over this catalyst, which is also shown by the lower SCR activity, compared to Ag/Al_2O_3.

Acknowledgments: This work has been financially supported by the Swedish Research Council and was performed within the Competence Centre for Catalysis, which is hosted by Chalmers University of Technology and financially supported by the Swedish Energy Agency and the member companies: AB Volvo, ECAPS AB, Haldor Topsøe A/S, Scania CV AB, Volvo Car Corporation AB and Wärtsilä Finland Oy.

Author Contributions: L.S., P.-A.C., M.S. and H.H. conceived and designed the experiments; L.S performed the experiments; L.S., P.-A.C., M.S. and H.H. analyzed the data; L.S., P.-A.C., M.S. and H.H. wrote the paper.

Conflicts of Interest: The authors declare no conflict of interest. The founding sponsors had no role in the design of the study; in the collection, analyses, or interpretation of data; in the writing of the manuscript, and in the decision to publish the results.

References

1. Wang, J.H.; Zhao, H.W.; Haller, G.; Li, Y.D. Recent advances in the selective catalytic reduction of NO_x with NH_3 on Cu-Chabazite catalysts. *Appl. Catal. B Environ.* **2017**, *202*, 346–354. [CrossRef]
2. Shishkin, A.; Shwan, S.; Pingel, T.N.; Olsson, E.; Clemens, A.; Carlsson, P.A.; Härelind, H.; Skoglundh, M. Functionalization of SSZ-13 and Fe-Beta with copper by NH_3 and NO facilitated solid-state ion-exchange. *Catalysts* **2017**, *7*, 232. [CrossRef]
3. Clemens, A.K.S.; Shishkin, A.; Carlsson, P.A.; Skoglundh, M.; Martinez-Casado, F.J.; Matej, Z.; Balmes, O.; Härelind, H. Reaction-driven ion exchange of copper into zeolite SSZ-13. *ACS Catal.* **2015**, *5*, 6209–6218. [CrossRef]
4. Gunnarsson, F.; Pihl, J.A.; Toops, T.J.; Skoglundh, M.; Härelind, H. Lean NO_x reduction over Ag/alumina catalysts via ethanol-SCR using ethanol/gasoline blends. *Appl. Catal. B Environ.* **2017**, *202*, 42–50. [CrossRef]
5. Matarrese, R.; Ingelsten, H.H.; Skoglundh, M. Aspects of reducing agent and role of amine species in the reduction of NO over H-ZSM-5 in oxygen excess. *J. Catal.* **2008**, *258*, 386–392. [CrossRef]
6. Chorkendorff, I.; Niemantsverdriet, J.W. *Concepts of Modern Catalysis and Kinetics*; WILEY-VCH Verlag GmbH & Co. KGaA: Weinheim, Germany, 2007.
7. Satokawa, S. Enhancing the $NO/C_3H_8/O_2$ reaction by using H_2 over Ag/Al_2O_3 catalysts under lean-exhaust conditions. *Chem. Lett.* **2000**, *29*, 294–295. [CrossRef]
8. Breen, J.P.; Burch, R.; Hardacre, C.; Hill, C.J. Structural investigation of the promotional effect of hydrogen during the selective catalytic reduction of NO_x with hydrocarbons over Ag/Al_2O_3 catalysts. *J. Phys. Chem. B* **2005**, *109*, 4805–4807. [CrossRef] [PubMed]
9. Satokawa, S.; Shibata, J.; Shimizu, K.; Atsushi, S.; Hattori, T. Promotion effect of H_2 on the low temperature activity of the selective reduction of NO by light hydrocarbons over Ag/Al_2O_3. *Appl. Catal. B Environ.* **2003**, *42*, 179–186. [CrossRef]
10. Kannisto, H.; Ingelsten, H.H.; Skoglundh, M. Aspects of the role of hydrogen in H_2-assisted HC-SCR over $Ag\text{-}Al_2O_3$. *Top. Catal.* **2009**, *52*, 1817. [CrossRef]

11. Shibata, J.; Takada, Y.; Shichi, A.; Satokawa, S.; Satsuma, A.; Hattori, T. Ag cluster as active species for SCR of NO by propane in the presence of hydrogen over Ag-MFI. *J. Catal.* **2004**, *222*, 368–376. [CrossRef]
12. Breen, J.P.; Burch, R. A review of the effect of the addition of hydrogen in the selective catalytic reduction of NO_x with hydrocarbons on silver catalysts. *Top. Catal.* **2006**, *39*, 53–58. [CrossRef]
13. Boutros, M.; Starck, J.; de Tymowski, B.; Trichard, J.-M.; Da Costa, P. On the effect of poor metals (Al, Ga, In) on the NO_x conversion in ethanol selective catalytic reduction. *Top. Catal.* **2009**, *52*, 1786. [CrossRef]
14. Li, J.H.; Hao, J.M.; Cui, X.Y.; Fu, L.X. Influence of preparation methods of In_2O_3/Al_2O_3 catalyst on selective catalytic reduction of NO by propene in the presence of oxygen. *Catal. Lett.* **2005**, *103*, 75–82. [CrossRef]
15. Maunula, T.; Kintaichi, Y.; Inaba, M.; Haneda, M.; Sato, K.; Hamada, H. Enhanced activity of in and Ga-supported sol-gel alumina catalysts for NO reduction by hydrocarbons in lean conditions. *Appl. Catal. B Environ.* **1998**, *15*, 291–304. [CrossRef]
16. Maunula, T.; Kintaichi, Y.; Haneda, M.; Hamada, H. Preparation and reaction mechanistic characterization of sol-gel indium/alumina catalysts developed for NO_x reduction by propene in lean conditions. *Catal. Lett.* **1999**, *61*, 121–130. [CrossRef]
17. Park, P.W.; Ragle, C.S.; Boyer, C.L.; Balmer, M.L.; Engelhard, M.; McCready, D. In_2O_3/Al_2O_3 catalysts for NO_x reduction in lean condition. *J. Catal.* **2002**, *210*, 97–105. [CrossRef]
18. Erkfeldt, S.; Petersson, M.; Palmqvist, A. Alumina-supported In_2O_3, Ga_2O_3 and B_2O_3 catalysts for lean NO_x reduction with dimethyl ether. *Appl. Catal. B Environ.* **2012**, *117*, 369–383. [CrossRef]
19. Doronkin, D.E.; Fogel, S.; Tamm, S.; Olsson, L.; Khan, T.S.; Bligaard, T.; Gabrielsson, P.; Dahl, S. Study of the "Fast SCR"-like mechanism of H_2-assisted SCR of NO_x with ammonia over Ag/Al_2O_3. *Appl. Catal. B Environ.* **2012**, *113*, 228–236. [CrossRef]
20. Ström, L.; Carlsson, P.-A.; Skoglundh, M.; Härelind, H. Hydrogen-assisted SCR of NO_x over alumina-supported silver and indium catalysts using C_2-hydrocarbons and oxygenates. *Appl. Catal. B Environ.* **2016**, *181*, 403–412. [CrossRef]
21. Tamm, S.; Vallim, N.; Skoglundh, M.; Olsson, L. The influence of hydrogen on the stability of nitrates during H_2-assisted SCR over Ag/Al_2O_3 catalysts—A drift study. *J. Catal.* **2013**, *307*, 153–161. [CrossRef]
22. Sadokhina, N.A.; Doronkin, D.E.; Baeva, G.N.; Dahl, S.; Stakheev, A.Y. Reactivity of surface nitrates in H_2-assisted SCR of NO_x over Ag/Al_2O_3 catalyst. *Top. Catal.* **2013**, *56*, 737–744. [CrossRef]
23. Kim, P.S.; Kim, M.K.; Cho, B.K.; Nam, I.-S.; Oh, S.H. Effect of H_2 on denox performance of HC-SCR over Ag/Al_2O_3: Morphological, chemical and kinetic changes. *J. Catal.* **2013**, *301*, 65–76. [CrossRef]
24. Thomas, C. On an additional promoting role of hydrogen in the H_2-assisted C_3H_6-SCR of NO_x on Ag/Al_2O_3: A lowering of the temperature of formation-decomposition of the organo-NO_x intermediates? *Appl. Catal. B Environ.* **2015**, *162*, 454–462. [CrossRef]
25. Kondratenko, E.V.; Kondratenko, V.A.; Richter, M.; Fricke, R. Influence of O_2 and H_2 on NO reduction by NH_3 over Ag/Al_2O_3: A transient isotopic approach. *J. Catal.* **2006**, *239*, 23–33. [CrossRef]
26. Burch, R.; Breen, J.P.; Meunier, F.C. A review of the selective reduction of NO_x, with hydrocarbons under lean-burn conditions with non-zeolitic oxide and platinum group metal catalysts. *Appl. Catal. B Environ.* **2002**, *39*, 283–303. [CrossRef]
27. Gunnarsson, F.; Granlund, M.Z.; Englund, M.; Dawody, J.; Pettersson, L.J.; Härelind, H. Combining HC-SCR over Ag/Al_2O_3 and hydrogen generation over Rh/CeO_2-ZrO_2 using biofuels: An integrated system approach for real applications. *Appl. Catal. B Environ.* **2015**, *162*, 583–592. [CrossRef]
28. Shimizu, K.; Shibata, J.; Yoshida, H.; Satsuma, A.; Hattori, T. Silver-alumina catalysts for selective reduction of NO by higher hydrocarbons: Structure of active sites and reaction mechanism. *Appl. Catal. B Environ.* **2001**, *30*, 151–162. [CrossRef]
29. Bogdanchikova, N.; Meunier, F.C.; Avalos-Borja, M.; Breen, J.P.; Pestryakov, A. On the nature of the silver phases of Ag/Al_2O_3 catalysts for reactions involving nitric oxide. *Appl. Catal. B Environ.* **2002**, *36*, 287–297. [CrossRef]
30. Iglesias-Juez, A.; Hungria, A.B.; Martinez-Arias, A.; Fuerte, A.; Fernandez-Garcia, M.; Anderson, J.A.; Conesa, J.C.; Soria, J. Nature and catalytic role of active silver species in the lean NO_x reduction with C_3H_6 in the presence of water. *J. Catal.* **2003**, *217*, 310–323. [CrossRef]
31. Kannisto, H.; Ingelsten, H.H.; Skoglundh, M. Ag-Al_2O_3 catalysts for lean NO_x reduction-influence of preparation method and reductant. *J. Mol. Catal. A Chem.* **2009**, *302*, 86–96. [CrossRef]

32. Shimizu, K.-I.; Satsuma, A. Reaction mechanism of H_2-promoted selective catalytic reduction of NO with NH_3 over Ag/Al_2O_3. *J. Phys. Chem. C* **2007**, *111*, 2259–2264. [CrossRef]
33. Shibata, J.; Shimizu, K.; Takada, Y.; Shichia, A.; Yoshida, H.; Satokawa, S.; Satsuma, A.; Hattori, T. Structure of active Ag clusters in Ag zeolites for SCR of NO by propane in the presence of hydrogen. *J. Catal.* **2004**, *227*, 367–374. [CrossRef]
34. Meunier, F.C.; Breen, J.P.; Zuzaniuk, V.; Olsson, M.; Ross, J.R.H. Mechanistic aspects of the selective reduction of NO by propene over alumina and silver-alumina catalysts. *J. Catal.* **1999**, *187*, 493–505. [CrossRef]
35. Tamm, S.; Fogel, S.; Gabrielsson, P.; Skoglundh, M.; Olsson, L. The effect of the gas composition on hydrogen-assisted NH_3-SCR over Ag/Al_2O_3. *Appl. Catal. B Environ.* **2013**, *136*, 168–176. [CrossRef]
36. Richter, M.; Fricke, R.; Eckelt, R. Unusual activity enhancement of NO conversion over Ag/Al_2O_3 by using a mixed NH_3/H_2 reductant under lean conditions. *Catal. Lett.* **2004**, *94*, 115–118. [CrossRef]
37. Kondratenko, V.A.; Bentrup, U.; Richter, M.; Hansen, T.W.; Kondratenko, E.V. Mechanistic aspects of N_2O and N_2 formation in no reduction by NH_3 over Ag/Al_2O_3: The effect of O_2 and H_2. *Appl. Catal. B Environ.* **2008**, *84*, 497–504. [CrossRef]
38. Poisson, R.; Brunelle, J.-P.; Nortier, P. *Catalyst Supports and Supported Catalysts. Theoretical and Applied Concepts*; Stiles, A.B., Ed.; Stoneham: Butterworth, Malasia, 1987; pp. 44–47.
39. Knozinger, H.; Ratnasamy, P. Catalytic aluminas—Surface models and characterization of surface sites. *Catal. Rev. Sci. Eng.* **1978**, *17*, 31–70. [CrossRef]
40. Digne, M.; Sautet, P.; Raybaud, P.; Euzen, P.; Toulhoat, H. Use of DFT to achieve a rational understanding of acid-basic properties of gamma-alumina surfaces. *J. Catal.* **2004**, *226*, 54–68. [CrossRef]
41. Sazama, P.; Capek, L.; Drobna, H.; Sobalik, Z.; Dedecek, J.; Arve, K.; Wichterlova, B. Enhancement of decane-SCR-NO_x over Ag/alumina by hydrogen. Reaction kinetics and in situ FTIR and UV-vis study. *J. Catal.* **2005**, *232*, 302–317. [CrossRef]
42. Shi, C.; Cheng, M.J.; Qu, Z.P.; Bao, X.H. Investigation on the catalytic roles of silver species in the selective catalytic reduction of NO_x with methane. *Appl. Catal. B Environ.* **2004**, *51*, 171–181. [CrossRef]
43. Miao, S.J.; Wang, Y.; Ma, D.; Zhu, Q.J.; Zhou, S.T.; Su, L.L.; Tan, D.L.; Bao, X.H. Effect of Ag+ cations on nonoxidative activation of methane to C_2-hydrocarbons. *J. Phys. Chem. B* **2004**, *108*, 17866–17871. [CrossRef]
44. Musi, A.; Massiani, P.; Brouri, D.; Trichard, J.-M.; Da Costa, P. On the characterisation of silver species for SCR of NO_x with ethanol. *Catal. Lett.* **2009**, *128*, 25–30. [CrossRef]
45. Sato, K.; Yoshinari, T.; Kintaichi, Y.; Haneda, M.; Hamada, H. Remarkable promoting effect of rhodium on the catalytic performance of Ag/Al_2O_3 for the selective reduction of NO with decane. *Appl. Catal. B Environ.* **2003**, *44*, 67–78. [CrossRef]
46. Männikkö, M.; Skoglundh, M.; Ingelsten, H.H. Selective catalytic reduction of NO_x with methanol over supported silver catalysts. *Appl. Catal. B Environ.* **2012**, *119*, 256–266. [CrossRef]
47. Pestryakov, A.N.; Davydov, A.A. Study of supported silver states by the method of electron spectroscopy of diffuse reflectance. *J. Electron Spectrosc. Relat. Phenom.* **1995**, *74*, 195–199. [CrossRef]
48. She, X.; Flytzani-Stephanopoulos, M. The role of AgOAl species in silver-alumina catalysts for the selective catalytic reduction of NO_x with methane. *J. Catal.* **2006**, *237*, 79–93. [CrossRef]
49. Lv, J.; Kako, T.; Li, Z.; Zou, Z.; Ye, J. Synthesis and photocatalytic activities of $NaNbO_3$ rods modified by In_2O_3 nanoparticles. *J. Phys. Chem. C* **2010**, *114*, 6157–6162. [CrossRef]
50. Yang, X.; Xu, J.; Wong, T.; Yang, Q.; Lee, C.-S. Synthesis of In_2O_3-In_2S_3 core-shell nanorods with inverted type-I structure for photocatalytic H_2 generation. *Phys. Chem. Chem. Phys.* **2013**, *15*, 12688–12693. [CrossRef] [PubMed]
51. Zhu, G.; Guo, L.; Shen, X.; Ji, Z.; Chen, K.; Zhou, H. Monodispersed In_2O_3 mesoporous nanospheres: One-step facile synthesis and the improved gas-sensing performance. *Sens. Actuators B Chem.* **2015**, *220*, 977–985. [CrossRef]
52. Zhang, F.; Li, X.; Zhao, Q.; Zhang, Q.; Tade, M.; Liu, S. Fabrication of α-Fe_2O_3/In_2O_3 composite hollow microspheres: A novel hybrid photocatalyst for toluene degradation under visible light. *J. Colloid Interface Sci.* **2015**, *457*, 18–26. [CrossRef] [PubMed]
53. Yin, J.Z.; Huang, S.B.; Jian, Z.C.; Pan, M.L.; Zhang, Y.Q.; Fei, Z.B.; Xu, X.R. Enhancement of the visible light photocatalytic activity of heterojunction $In_2O_3/BiVO_4$ composites. *Appl. Phys. A Mater. Sci. Process.* **2015**, *120*, 1529–1535. [CrossRef]

54. Liu, Q.; Zhang, W.; Liu, R.; Mao, G. Controlled synthesis of monodispersed sub-50 nm nanoporous In_2O_3 spheres and their photoelectrochemical performance. *Eur. J. Inorg. Chem.* **2015**, *2015*, 845–851. [CrossRef]
55. Morterra, C.; Magnacca, G. A case study: Surface chemistry and surface structure of catalytic aluminas, as studied by vibrational spectroscopy of adsorbed species. *Catal. Today* **1996**, *27*, 497–532. [CrossRef]
56. Hadjiivanov, K.I. Identification of neutral and charged N_xO_y surface species by IR spectroscopy. *Catal. Rev. Sci. Eng.* **2000**, *42*, 71–144. [CrossRef]
57. Underwood, G.M.; Miller, T.M.; Grassian, V.H. Transmission FT-IR and knudsen cell study of the heterogeneous reactivity of gaseous nitrogen dioxide on mineral oxide particles. *J. Phys. Chem. A* **1999**, *103*, 6184–6190. [CrossRef]
58. Satsuma, A.; Shimizu, K. In situ FT/IR study of selective catalytic reduction of NO over alumina-based catalysts. *Prog. Energy Combust. Sci.* **2003**, *29*, 71–84. [CrossRef]
59. Adams, E.C.; Skoglundh, M.; Gabrielsson, P.; Carlsson, P.A. Passive SCR: The effect of H_2 to NO ratio on the formation of NH_3 over alumina supported platinum and palladium catalysts. *Top. Catal.* **2016**, *59*, 970–975. [CrossRef]
60. Adams, E.C.; Skoglundh, M.; Folic, M.; Bendixen, E.C.; Gabrielsson, P.; Carlsson, P.-A. Ammonia formation over supported platinum and palladium catalysts. *Appl. Catal. B Environ.* **2015**, *165*, 10–19. [CrossRef]
61. Acke, F.; Westerberg, B.; Skoglundh, M. Selective reduction of no by HNCO over PT promoted Al_2O_3. *J. Catal.* **1998**, *179*, 528–536. [CrossRef]
62. Centeno, M.A.; Carrizosa, I.; Odriozola, J.A. In situ drifts study of the SCR reaction of NO with NH_3 in the presence of O_2 over lanthanide doped V_2O_5/Al_2O_3 catalysts. *Appl. Catal. B Environ.* **1998**, *19*, 67–73. [CrossRef]
63. Wallin, M.; Grönbeck, H.; Spetz, A.L.; Skoglundh, M. Vibrational study of ammonia adsorption on Pt/SiO_2. *Appl. Surf. Sci.* **2004**, *235*, 487–500. [CrossRef]
64. Yu, L.; Zhong, Q.; Zhang, S. The enhancement for SCR of NO by NH_3 over the H_2 or CO pretreated Ag/gamma-Al_2O_3 catalyst. *Phys. Chem. Chem. Phys.* **2014**, *16*, 12560–12566. [CrossRef] [PubMed]
65. Tamm, S. The role of silver for the H_2-effect in H_2-assisted selective catalytic reduction of NO_x with NH_3 over Ag/Al_2O_3. *Catal. Lett.* **2013**, *143*, 957–965. [CrossRef]
66. Anderson, J.R.; Pratt, K.C. *Introduction to Characterization and Testing of Catalysts*; Academic Press Inc.: Melbourne, Australia, 1985.
67. Kannisto, H.; Karatzas, X.; Edvardsson, J.; Pettersson, L.J.; Ingelsten, H.H. Efficient low temperature lean NO_x reduction over Ag/Al_2O_3—A system approach. *Appl. Catal. B Environ.* **2011**, *104*, 74–83. [CrossRef]
68. Wang-Hansen, C.; Kamp, C.J.; Skoglundh, M.; Andersson, B.; Carlsson, P.-A. Experimental method for kinetic studies of gas-solid reactions: Oxidation of carbonaceous matter. *J. Phys. Chem. C* **2011**, *115*, 16098–16108. [CrossRef]